

Biological evaluation of non-steroidal anti-inflammatory drugs-cobalt(II) complexes†

Filitsa Dimiza,^a Athanasios N. Papadopoulos,^b Vassilis Tangoulis,^a Vassilis Psycharis,^c Catherine P. Raptopoulou,^c Dimitris P. Kessissoglou^a and George Psomas^{*a}

Received 5th January 2010, Accepted 15th March 2010

First published as an Advance Article on the web 6th April 2010

DOI: 10.1039/b927472c

Cobalt(II) complexes with the non-steroidal anti-inflammatory drug mefenamic acid in the presence or absence of nitrogen donor heterocyclic ligands (2,2'-bipyridine, 1,10-phenanthroline or pyridine) have been synthesized and characterized with physicochemical and spectroscopic techniques. The experimental data suggest that mefenamic acid acts as deprotonated monodentate ligand coordinated to Co(II) ion through a carboxylato oxygen. The crystal structures of tetrakis(methanol)bis-(mefenamato)cobalt(II), **1** and (2,2'-bipyridine)bis(methanol)bis(mefenamato)cobalt(II), **2** have been determined by X-ray crystallography. The EPR spectra of complexes **1** and **2** in frozen solution reveal that they retain their structures. UV study of the interaction of the complexes with calf-thymus DNA (CT DNA) has shown that the complexes can bind to CT DNA and bis(methanol)bis(pyridine)bis-(mefenamato)cobalt(II) exhibits the highest binding constant. Competitive study with ethidium bromide (EB) has shown that the complexes can displace the DNA-bound EB indicating that they bind to DNA in strong competition with EB. The cyclic voltammograms of the complexes recorded in dmsO solution and in the presence of CT DNA in 1 : 2 dmsO : buffer (containing 150 mM NaCl and 15 mM trisodium citrate at pH 7.0) solution have shown that they can bind to CT DNA by the intercalative binding mode. Mefenamic acid and its cobalt(II) complexes exhibit good binding propensity to human or bovine serum albumin protein having relatively high binding constant values. The antioxidant activity of the compounds has been evaluated indicating their high scavenging activity against hydroxyl free radicals and superoxide radicals.

Introduction

Non-steroidal anti-inflammatory drugs (NSAIDs‡) are among the most frequently used medicinal drugs and they are utilized primarily as analgesic, anti-inflammatory and antipyretic agents since their side-effects have been well studied.¹ Their mode of action is either through inhibition of the cyclo-oxygenase(COX)-mediated production of prostaglandins or *via* COX-independent mechanisms by modulating cell proliferation and cell death in

cultured colon cancer cells lacking COX.² NSAIDs have presented chemopreventive and antitumorigenic activity by reducing the number and size of carcinogen-induced colon tumors and exhibiting a synergistic role on the activity of certain antitumor drugs.³ In an attempt to explain the tentative anticancer as well as the anti-inflammatory activity of the NSAIDs, their interaction with DNA should be of great interest.⁴ Nevertheless, the anionic form they present at physiological pH is an obstacle to their approach to the poly-anionic DNA backbone resulting in few reports on the interaction of NSAIDs and their complexes with DNA.⁵ Additionally, metal complexes have also exhibited synergistic activity when administered in conjunction with NSAIDs.⁶ It has been found that the copper complexes of some antiarthritic drugs are more active as anti-inflammatory agents than their parent compounds.⁷

Mefenamic acid (Hmef = 2-[(2,3-dimethylphenyl)-amino]-benzoic acid or N-(2,3-xylyl)anthranilic acid), (Fig. 1), is a NSAID that belongs to the derivatives of N-phenylanthranilic acid. It chemically resembles tolfenamic and flufenamic acids and other fenamates in clinical use. In the literature, the crystal structures of two tin(IV), a mononuclear and a dinuclear Cu(II) complexes of mefenamic acid have been reported.⁸

Cobalt is an element of biological interest. Its biological role is mainly focused on its presence in the active center of vitamin B12, which regulates indirectly the synthesis of DNA. Additionally, there are at least eight cobalt-dependent proteins.⁹ Cobalt is involved in the co-enzyme of vitamin B12 used as a

^aDepartment of General and Inorganic Chemistry, Faculty of Chemistry, Aristotle University of Thessaloniki, P.O. Box 135, GR-54124, Thessaloniki, Greece. E-mail: gepsomas@chem.auth.gr; Fax: +30+2310997738; Tel: +30+2310997790

^bDepartment of Nutrition and Dietetics, Faculty of Food Technology and Nutrition, Alexandrion Technological Educational Institution, Sindos, Thessaloniki, Greece

^cInstitute of Materials Science, NCSR "Demokritos", GR-15310, Aghia Paraskevi Attikis, Greece

† Electronic supplementary information (ESI) available: Additional data. CCDC reference numbers 759764 and 759765. For ESI and crystallographic data in CIF or other electronic format see DOI: 10.1039/b927472c

‡ Abbreviations: ABTS = 2,2'-azino-bis(3-ethylbenzothiazoline-6-sulfonic acid) radical cation, BHT = butylated hydroxytoluene, bipy = 2,2'-bipyridine, BSA = bovine serum albumin, COX = cyclo-oxygenase, CT = calf-thymus, DPPH = 1,1-diphenyl-picrylhydrazyl, EB = ethidium bromide, Hmef = mefenamic acid, HSA = human serum albumin, NDGA = nordihydroguaiaretic acid, NSAID = Non-steroidal anti-inflammatory drug, phen = 1,10-phenanthroline, py = pyridine, TEAP = Tetraethylammonium perchlorate, Trolox = 6-hydroxy-2,5,7,8-tetramethylchromane-2-carboxylic acid

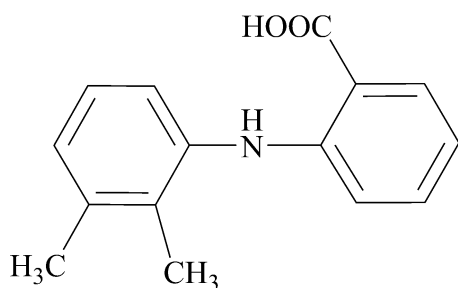


Fig. 1 Mefenamic acid (Hmef = 2-[(2,3-dimethylphenyl)-amino]benzoic acid).

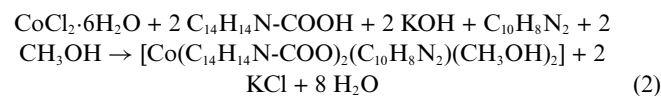
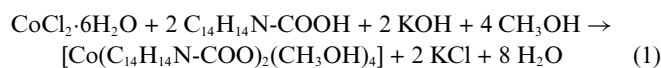
supplement of the vitamin.¹⁰ Since the first reported studies into the biological activity of Co complexes in 1952,¹¹ many cobalt complexes of biological interest have been reported with the most structurally characterized showing antitumor, antiproliferative,¹² antimicrobial,¹³ antifungal¹⁴ and antiviral¹⁵ activity. To the best of our knowledge, no cobalt(II) complexes of the NSAID group of N-phenylantranilic acids have been structurally characterized yet.

Our studies have been focused on the coordination chemistry of carboxylate-containing herbicides,¹⁶ antimicrobial¹⁷ or anti-inflammatory¹⁸ agents with metal ions in an attempt to examine their mode of binding and possible biological relevance. In addition, we have reported studies on the interaction of metal complexes with nucleic acids and their biological activity. Taking into consideration the reported biological role and activity of cobalt and its complexes as well as the significance of the NSAIDs in medicine, we have initiated the investigation of the interaction of cobalt(II) with ligands that belong to the NSAID group. In this context, we report the synthesis, the structural characterization, the electrochemical and the biological properties of the neutral mononuclear cobalt(II) complexes with the NSAID mefenamic acid in the absence ($[\text{Co}(\text{mef})_2(\text{MeOH})_4] \cdot 2\text{MeOH}$, **1-2MeOH**) or presence of a nitrogen-donor heterocyclic ligand such as bipy, phen or pyridine (py) ($[\text{Co}(\text{mef})_2(\text{bipy})(\text{MeOH})_2]$ **2**, $[\text{Co}(\text{mef})_2(\text{phen})(\text{MeOH})_2]$ **3** and $[\text{Co}(\text{mef})_2(\text{py})_2(\text{MeOH})_2]$ **4**). The crystal structures of **1-2MeOH** and **2** have been determined by X-ray crystallography. The study of the biological properties of the compounds has been focused on (i) the binding properties with CT DNA investigated with UV spectroscopy, cyclic voltammetry and competitive binding studies with ethidium bromide (EB), (ii) the affinity for bovine (BSA) and human serum albumin (HSA), proteins involved in the transport of metal ions and metal complexes with drugs through the blood stream, investigated with fluorescence spectroscopy and (iii) the antioxidant capacity, since the use of NSAIDs in medicine as analgesics and antiinflammatories may be related to free radicals scavenging.

Results and discussion

Synthesis and characterization of the complexes

The synthesis of the complexes in high yield was achieved *via* the aerobic reaction of mefenamic acid ($\text{C}_{14}\text{H}_{14}\text{N-COOH}$) and KOH with $\text{CoCl}_2 \cdot 6\text{H}_2\text{O}$ in the absence, (eqn (1)) for **1**, or presence of the corresponding N-donor heterocyclic ligand, *e.g.* ($\text{C}_{10}\text{H}_8\text{N}_2$, eqn (2)) for **2**, according to the equations:



The complexes are soluble in dmsO and dmf, stable in air and no electrolytes in dmsO.

In the IR spectrum, the observed absorption bands at 3370 (br,m) cm^{-1} , 1655 (s) cm^{-1} and 1255 (s) cm^{-1} attributed to the stretching vibrations $\nu(\text{H-O})$, $\nu(\text{C=O})_{\text{carboxylic}}$ and $\nu(\text{C-O})_{\text{carboxylic}}$, respectively, of the carboxylic moiety ($-\text{COOH}$) of the mefenamic acid, have been replaced in the IR spectra of the complexes by two very strong characteristic bands in the range 1609–1615 cm^{-1} and 1382–1389 cm^{-1} assigned as anti-symmetric, $\nu_{\text{asym}}(\text{C=O})$, and symmetric, $\nu_{\text{sym}}(\text{C=O})$, stretching vibrations of the carboxylato group, respectively. The difference $\Delta[\nu_{\text{asym}}(\text{C=O}) - \nu_{\text{sym}}(\text{C=O})]$, a useful characteristic tool for determining the coordination mode of the carboxylato ligands, gives a value falling in the range 224–230 cm^{-1} indicative of a monodentate coordination mode for the mefenamato ligand.^{18c}

The UV-vis spectra of the complexes have been recorded as nujol mull and in dmsO solution and are similar, suggesting that the complexes retain their structure in solution. In the visible region, three low-intensity bands are observed and can be assigned to d-d transitions. More specifically, for local O_h symmetry, band I observed in the region 733–742 nm may be attributed to a ${}^4\text{T}_{1g}(\text{F}) \rightarrow {}^4\text{T}_{2g}$ transition, band II in the region 535–565 nm to a ${}^4\text{T}_{2g}(\text{F}) \rightarrow {}^4\text{A}_{2g}$ transition and band III at 440–475 nm to a ${}^4\text{T}_{1g}(\text{F}) \rightarrow {}^4\text{T}_{1g}(\text{P})$ transition and are typical for distorted octahedral high-spin Co^{2+} complexes.⁹ Additionally, an absorption band assigned to charge transfer transition for the mefenamato ligand exists at around 395 nm.

The observed values of μ_{eff} (4.35–4.50 BM) for the complexes at room temperature are higher than the spin-only value (3.87 MB) showing spin-orbit coupling due to $t_{2g}^5 e_g^2$ electron configuration. The values are within the range reported for mononuclear high-spin $\text{Co}(\text{II})$ complexes ($S = 3/2$).⁹

X-Band EPR measurements were carried out in powder samples as well as in frozen solutions of **1** and **2** in dmsO and are shown in Fig. S1.† As a consequence of the fast spin-lattice relaxation time of high-spin $\text{Co}(\text{II})$, signals were observed only below 70 K. For the powder spectra, at temperatures $T < 25$ K, **1** exhibits a broad derivative and an axial broad peak with $g_1 = 3.9(1)$ and $g_2 = 2.04(1)$ while **2** exhibits a rhombic broad signal with three g values $g_1 = 5.5(1)$, $g_2 = 3.5(1)$ and $g_3 = 3.0(1)$, ($g_{\text{iso}} = 4.0$) and a weak signal centred also at $g = 2.04(1)$. The frozen solutions of both systems are more isotropic as it is expected with axial g -values: $g_1 = 4.0(1)$, $g_2 = 2.02(1)$ revealing that the systems do retain their structures.

The dominant broadening effect emerges when the g -strain is converted into B -strain through the equation $\Delta B = -\left(\frac{h\nu}{\mu_B}\right)\left(\frac{\Delta g}{g^2}\right)$, where the parameters have their usual meaning. Thus, the largest and smallest g -values of the powder and solution spectra have field widths that differ by an order of magnitude, thereby rationalizing the broad high-field features of the spectrum.¹⁹

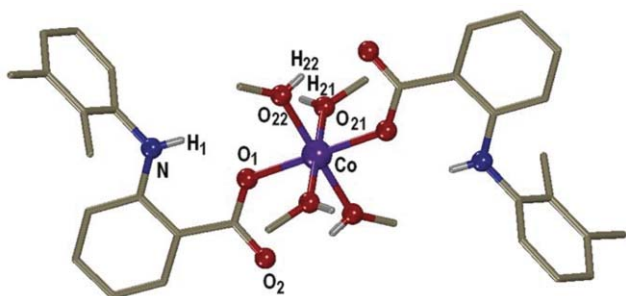
Table 1 Selected bond distances and angles for complex **1**

Bond distances/Å		Bond distances/Å	
Co–O(1)	2.060(2)	C(21)–O(21)	1.377(6)
Co–O(21)	2.084(3)	C(22)–O(22)	1.305(5)
Co–O(22)	2.063(3)	C(1)–O(1)	1.267(4)
C(1)–O(2)	1.254(4)		
Bond angles/°		Bond angles/°	
O(1)–Co–O(22)	90.2(1)	O(1)–Co–O(21)	90.6(1)
O(1)–Co–O(22)′	89.8(1)	O(1)′–Co–O(21)	89.4(1)
O(21)–Co–O(22)	88.2(2)	O(21)–Co–O(22)′	91.8(2)
O(1)–Co–O(1)′	180.0	O(21)–Co–O(21)′	180.0
O(22)–Co–O(22)′	180.0		

Primed atoms are generated by symmetry: (′) $-x, 1-y, -z$.

Crystal structure of [Co(mef)₂(MeOH)₄·2MeOH, 1-2MeOH

A diagram of **1** is shown in Fig. 2, and selected bond distances and angles are listed in Table 1. The complex is mononuclear with the mefenamato ligand behaving as a monodentate deprotonated ligand coordinated to cobalt atom *via* a carboxylate oxygen.

**Fig. 2** The molecular structure and partial labeling of **1** with only the heteroatoms labeled.

The structure of the complex is centrosymmetric, the cobalt(II) ion is sitting on a center of symmetry and is coordinated to two mefenamato ligands and four methanol molecules related by the inversion center. Thus, the cobalt atom is six-coordinate and it displays an octahedral geometry. All the Co–O distances are of the same magnitude with Co–O_{carboxylate} being the shortest (Co–O(1) = 2.060(2) Å) and the inequivalent Co–O_{methanol} (Co–O(21) 2.084(3), Co–O(22) = 2.063(3) Å) being the longest. Taking into account the small differences found in the Co–O distances in combination with the angles around cobalt (O(1)–Co–O(22) = 90.2(1)°, O(1)–Co–O(21) = 90.6(1)° and O(21)–Co–O(22) = 88.2(2)°, the octahedron displays a slight distortion. The carboxylate group is asymmetrically bound to cobalt (C(1)–O(1) = 1.267(4) Å and C(1)–O(2) = 1.254(4) Å).

Crystal structure of [Co(mef)₂(bipy)(MeOH)₂], **2**

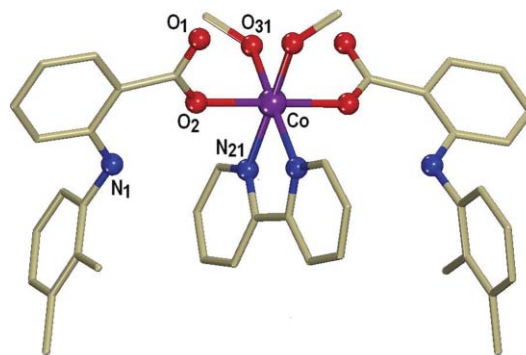
A diagram of **2** is shown in Fig. 3, and selected bond distances and angles are listed in Table 2. The complex is mononuclear and the mefenamato ligand behaves as a monodentate deprotonated ligand coordinated to cobalt atom *via* a carboxylate oxygen.

The cobalt atom is six-coordinate and is surrounded by two mefenamato ligands, two methanol molecules and a bidentate 2,2′-bipyridine ligand showing a distorted octahedral geometry. The two nitrogen atoms of bipy and two oxygen atoms of the methanol

Table 2 Selected bond distances and angles for complex **2**

Bond distances/Å		Bond distances/Å	
Co–O(2)	2.063(2)	Co–O(31)	2.072(3)
Co–N(21)	2.115(3)	C(1)–O(1)	1.244(4)
C(1)–O(2)	1.257(4)		
Bond angles/°		Bond angles/°	
O(2)–Co–O(2)′	179.6(2)	O(2)–Co–N(21)	92.7(1)
O(2)–Co–O(31)	88.0(2)	O(2)–Co–N(21)′	87.0(1)
O(2)–Co–O(31)′	92.3(1)	O(31)–Co–N(21)	96.4(2)
O(31)–Co–N(21)′	171.5(2)	O(31)–Co–O(31)′	90.6(3)
N(21)–Co–N(21)′	77.0(2)		

Primed atoms are generated by symmetry: (′) $-x, y, -z$.

**Fig. 3** The molecular structure and partial labeling of **2** with only the heteroatoms labeled.

molecules form the basal plane of the octahedron with the two oxygen atoms from the mefenamato ligands lying at the apical.

The bond distances around the cobalt atom are not equal, with the coordinated carboxylate oxygen atoms (Co–O(2) = 2.064(2) Å) lying closer to Co than the methanol oxygen atoms (Co–O(31) = 2.072(3) Å) and the bipy nitrogen atoms (Co–N(21)) being at a distance 2.115(3) Å. The methanol molecules are lying at *cis* positions (O(31)–Co–O(31)′ = 90.6(3)°) and the mefenamato oxygen atoms are *trans* (O(2)–Co–O(2)′ = 179.6(2)°) to each other. The carboxylate group is asymmetrically bound to cobalt (C(1)–O(2) = 1.257(4) Å and C(1)–O(1) = 1.244(4) Å).

The N(21)–Co–N(21)′ angle observed is 77.0(2)° and is similar to reported values of other chelating polycyclic diimines.²⁰ The 2,2′-bipyridine ligand is planar with the cobalt atom lying in this plane.

The crystal structures of **1** and **2** are the only structures of Co(II)-anthranilic acid complexes reported. Generally structurally characterized metal complexes of mefenamic acid or flufenamic, tolfenamic, niflumic and meclofenamic acid, members of the NSAID group of anthranilic acids are rare, with only copper(II) and tin(II) complexes reported so far (Table 3).²¹

Interaction with DNA

Transition metal complexes can bind to DNA *via* both covalent and/or non-covalent interactions. In the case of covalent binding, the labile ligand of the complexes can be replaced by a nitrogen base of DNA such as guanine N7, while the non-covalent DNA interactions include intercalative, electrostatic and groove (surface) binding of metal complexes outside of DNA helix, along major or minor groove.²² To the best of our knowledge, metal

Table 3 X-Ray structurally characterized complexes of NSAID group of anthranilic acids

Metal	Complex	Geometry	Reference
Cu	[Cu ₂ (fluf) ₄ (caffeine)(H ₂ O)]	Paddlewheel	21a
Cu	[Cu(nifl) ₂ (DMSO) ₂]	Paddlewheel	7a
Cu	[Cu ₂ (nifl) ₄ (H ₂ O) ₂]	Paddlewheel	21b
Cu	[Cu(tolf) ₂ (DMF) ₂]	Paddlewheel	21c
Cu	[Cu(mef) ₂ (DMSO) ₂]	Paddlewheel	8c
Cu	[Cu(nifl) ₂ (3-pyridylmethanol) ₂]	Square-planar	21d
Cu	[Cu(fluf) ₂ (Et ₂ nia) ₂ (H ₂ O) ₂]	Octahedral	21e
Cu	[Cu(mef) ₂ (MeOH) ₂ (py) ₂]	Octahedral	8b
Sn	[Me ₂ (fluf)SnOSn(fluf)Me ₂]	Octahedral	21f
Sn	[Bu ₂ Sn(tolf)O(tolf)SnBu ₂]	Distorted trigonal bipyramidal	21g
Sn	[Me ₂ Sn(mef)O(mef)SnMe ₂]	Distorted trigonal bipyramidal	8a
Sn	[Bu ₂ Sn(mef)O(mef)SnBu ₂]	Distorted trigonal bipyramidal	8a
Co	[Co(mef) ₂ (MeOH) ₄]·MeOH	Octahedral	This work
Co	[Co(mef) ₂ (bipy)(MeOH) ₂]	Octahedral	This work

Hfluf = flufenamic acid, Hnifl = niflumic acid, Htolf = tolfenamic acid, Hmef = mefenamic acid, Et₂nia = N,N-diethylnicotinamide.

complexes of the oxicam NSAIDs have been found to bind to DNA *via* the intercalative mode,^{5b} while the interaction of DNA with metal complexes of the anthranilic acid NSAIDs has not been investigated yet.

Study of the DNA-binding with UV spectroscopy

The changes observed in the UV spectra upon titration may give evidence of the existing interaction mode, since a hypochromism due to $\pi \rightarrow \pi^*$ stacking interactions may appear in the case of the intercalative binding mode, while a red-shift (bathochromism) may be observed when the DNA duplex is stabilized.²³

The UV spectra have been recorded for a constant CT DNA concentration in different [compound]/[DNA] mixing ratios (*r*). UV spectra of CT DNA in the presence of a compound derived for diverse *r* values are shown representatively for **2** in Fig. 4. Hmef and the complexes exhibit similar behaviour upon their addition on CT DNA solution. The decrease of the intensity at $\lambda_{\max} = 258$ nm is accompanied by a red-shift of the λ_{\max} up to 265 nm for all compounds, indicating that the interaction with CT DNA results in the direct formation of a new complex with double-helical CT DNA.²² The observed hypochromism could be attributed to

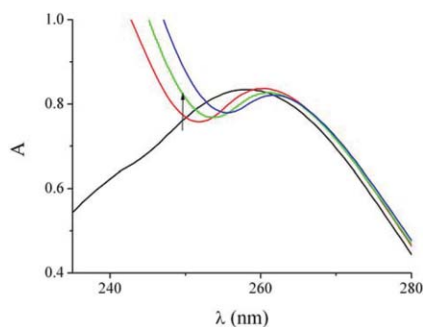


Fig. 4 (A) UV spectra of CT DNA in buffer solution (150 mM NaCl and 15 mM trisodium citrate at pH 7.0) in the absence or presence of [Co(mef)₂(bipy)(MeOH)₂]**2**. The arrows show the changes upon increasing amounts of complex.

stacking interaction between the aromatic chromophore (either from mefenamato and/or the N-donor ligands) of the complexes and DNA base pairs consistent with the intercalative binding mode, while the red-shift is an evidence of the stabilization of the CT DNA duplex.²³

The changes occurring in the spectrum of a 10⁻⁵ M solution of Hmef, **1** and **4** upon addition of CT DNA in diverse *r* values can be observed in Fig. 5. In the UV region, the intense absorption bands observed in the spectra of the complexes are attributed to the intraligand transition of the coordinated groups of mefenamato ligands. Any interaction between each complex and CT DNA could perturb its intraligand centred spectral transitions.²⁴

In the UV spectrum of Hmef, no significant changes were observed in the position of the $\pi \rightarrow \pi^*$ transition bands upon addition of CT DNA (Fig. 5(A)). On the other hand, the intensity of the bands centred at 324 nm is increased upon addition of CT DNA, suggesting tight binding to CT DNA. The observed hyperchromic effect suggests binding to CT DNA ascribed either to external contact or to the fact that mefenamic acid could uncoil the helix structure of DNA.²⁵

In the UV spectrum of **1** (Fig. 5(B)), the band centred at 340 nm exhibits a hyperchromism accompanied by a red-shift of 3 nm (up to 343 nm) suggesting probable external binding to DNA and stabilization. Additionally, the band at 300 nm presents a hyperchromism accompanied by a blue-shift of 4 nm (up to 296 nm).

In the UV spectrum of **4**, the band centred at 340 nm exhibits initially a slight hypochromism (Fig. 5(C)) suggesting tight binding to CT DNA probably by intercalation. Further addition of DNA results in a hyperchromism accompanied by a red-shift of 4 nm (up to 343 nm) suggesting tight binding and stabilization. Additionally, the band at 300 nm presents a hyperchromism accompanied by a red-shift of 5 nm (up to 305 nm). A distinct isosbestic point at 331 nm appears upon addition of CT DNA. The behaviour of complexes **2** and **3** is quite similar to that of **4**.

The results derived from the UV titration experiments suggest that all compounds can bind to CT DNA although the exact mode of binding cannot be merely proposed by UV spectroscopic titration studies.²⁶ Nevertheless, the existence of hypochromism for complexes **2–4** could be considered as evidence that the binding of the complexes involving intercalation between the base pairs of CT DNA cannot be ruled out.^{17b–d} The different behaviour between complexes **2–4** and **1** may be attributed either to the steric effect due to pyridine ligands in complex **4** or to a combination of steric and chelate effects provided by the bipy or phen ligands in **2** and **3**, respectively.

The binding constant of the compounds to CT DNA, K_b , can be obtained by the ratio of the slope to the *y* intercept in plots $\frac{[DNA]}{(\epsilon_A - \epsilon_f)}$ versus [DNA] (insets in Fig. 5(B) and (C)), according to the equation:^{23b}

$$\frac{[DNA]}{(\epsilon_A - \epsilon_f)} = \frac{[DNA]}{(\epsilon_b - \epsilon_f)} + \frac{1}{K_b(\epsilon_b - \epsilon_f)} \quad (3)$$

where [DNA] is the concentration of DNA in base pairs, $\epsilon_A = A_{\text{obsd}}/[\text{compound}]$, ϵ_f = the extinction coefficient for the free compound and ϵ_b = the extinction coefficient for the compound in

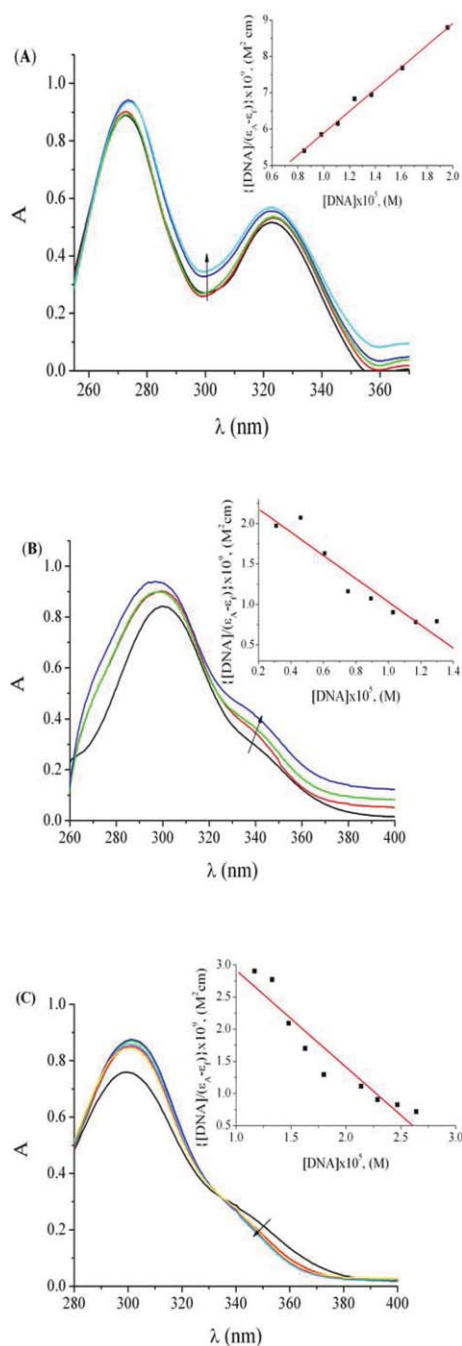


Fig. 5 UV spectra of ([compound] = 1×10^{-5} M) (A) Hmf, (B) $[\text{Co}(\text{mef})_2(\text{MeOH})_4]$ **1** and (C) $[\text{Co}(\text{mef})_2(\text{py})_2(\text{MeOH})_2]$ **4** in dmsol solution in the presence of CT DNA at increasing amounts. The arrows show the changes upon increasing amounts of CT DNA. Inset: plot of $\frac{[\text{DNA}]}{(\Delta A - \Delta_f)}$ versus $[\text{DNA}]$.

the fully bound form. The calculated K_b values (Table 4) suggest a relatively strong binding of Hmf and complexes **1–4** to CT DNA^{17b-f} and increase in the order $3 < 2 < 1 < \text{Hmf} < 4$ with complex **4** exhibiting the highest K_b value ($3.22 (\pm 0.04) \times 10^5 \text{ M}^{-1}$). The coordination of Hmf to Co(II) results in a decrease of the K_b value as calculated for **1** (Table 4), while the co-existence of the N,N'-donor heterocyclic ligands leads to lower K_b values as for **2**

Table 4 The DNA binding constants (K_b) and the Stern–Volmer constants (K_{SV}) of complexes **1–4**

Complex	K_b/M^{-1}	K_{SV}/M^{-1}
Hmf	$1.05 (\pm 0.02) \times 10^5$	$1.58 (\pm 0.06) \times 10^5$
$[\text{Co}(\text{mef})_2(\text{MeOH})_4]$, 1	$5.82 (\pm 0.25) \times 10^4$	$7.63 (\pm 0.42) \times 10^5$
$[\text{Co}(\text{mef})_2(\text{bipy})(\text{MeOH})_2]$, 2	$4.59 (\pm 0.24) \times 10^4$	$1.09 (\pm 0.03) \times 10^6$
$[\text{Co}(\text{mef})_2(\text{phen})(\text{MeOH})_2]$, 3	$3.02 (\pm 0.45) \times 10^4$	$4.10 (\pm 0.22) \times 10^5$
$[\text{Co}(\text{mef})_2(\text{py})_2(\text{MeOH})_2]$, 4	$3.22 (\pm 0.04) \times 10^5$	$2.17 (\pm 0.09) \times 10^5$

and **3**, indicating that the existence of a N,N'-donor ligand does not enhance the affinity for DNA. On the other hand, the presence of the N-donor ligand pyridine results to increased affinity for DNA. Finally, the K_b values of all compounds are of the same magnitude to that of the classical intercalator EB ($K_b = 1.23 (\pm 0.07) \times 10^5 \text{ M}^{-1}$).^{16c,17d}

Competitive studies with ethidium bromide

Ethidium bromide (EB = 3,8-diamino-5-ethyl-6-phenyl-phenanthridinium bromide) is a typical indicator of intercalation since it can form soluble complexes with nucleic acids emitting intense fluorescence in the presence of CT DNA due to the intercalation of the planar phenanthridinium ring between adjacent base pairs on the double helix. The changes observed in the fluorescence spectra of EB on its binding to CT DNA are often used for the interaction study between DNA and other compounds, such as metal complexes.²⁷

Hmf and complexes **1–4** show no fluorescence at room temperature in solution or in the presence of CT DNA, and their binding to DNA cannot be directly predicted through emission spectra. Hence, competitive EB binding studies may be undertaken in order to examine the binding of each compound with DNA. EB does not show any appreciable emission in buffer solution due to fluorescence quenching of the free EB by the solvent molecules and the fluorescence intensity is highly enhanced upon addition of CT DNA, due to its strong intercalation with DNA base pairs. Addition of a second molecule, which may bind to DNA more strongly than EB results to a decrease the DNA-induced EB emission. Two mechanisms have been proposed to account for this reduction in the emission intensity: the replacement of EB, and/or electron transfer.²⁸

The emission spectra of EB bound to CT DNA in the absence and presence of each compound have been recorded for $[\text{EB}] = 20 \mu\text{M}$ and $[\text{DNA}] = 26 \mu\text{M}$ upon addition of increasing amounts of each compound. The addition of Hmf or each complex **1–4** at diverse r values (Fig. 6(A)) results in a significant decrease of the intensity of the emission band of the DNA-EB system at 592 nm (up to 20% of the initial EB-DNA fluorescence intensity for Hmf, 14% for **1**, 19% for **2**, 26% for **3** and 23% for **4**) indicating the competition of the complexes with EB in binding to DNA. The observed significant quenching of DNA-EB fluorescence for Hmf and **1–4** suggests that they displace EB from the DNA-EB complex and they probably interact with CT DNA by the intercalative mode.^{17b-f,29}

The Stern–Volmer constant, K_{SV} , can be obtained by the slope of the diagram $\frac{I_0}{I}$ versus $[\text{Q}]$ and is used to evaluate the quenching efficiency for each compound according to the equation (eqn (4)):

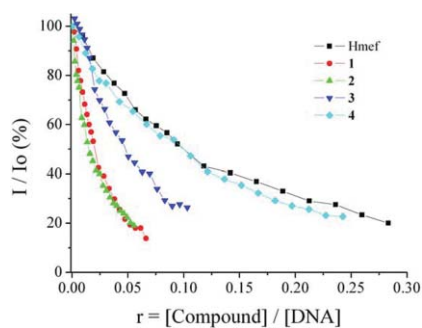


Fig. 6 Plot of EB relative fluorescence intensity at $\lambda_{em} = 592$ nm (%) versus r ($r = [\text{complex}]/[\text{DNA}]$) for Hmef and complexes **1–4** in buffer solution (150 mM NaCl and 15 mM trisodium citrate at pH 7.0).

$$\frac{I_0}{I} = 1 + K_{SV}[Q] \quad (4)$$

where I_0 and I are the emission intensities in the absence and the presence of the quencher, respectively, $[Q]$ is the concentration of the quencher (Hmef or complexes **1–4**). The Stern–Volmer plots of DNA-EB (Fig. S2†) illustrate that the quenching of EB bound to DNA by the compounds is in good agreement ($R = 0.99$) with the linear Stern–Volmer equation (eqn (4)), which proves that the partial replacement of EB bound to DNA by each compound results in a decrease of the fluorescence intensity. The high K_{SV} values of the compounds (Table 4) show that they bind tightly to the DNA.^{17b–f}

Study of the DNA-binding with cyclic voltammetry

The cyclic voltammograms of **4** in dmsO solution (Fig. 7) exhibit one cathodic wave at -920 mV (E_{pc1}) followed by two anodic waves at -10 mV (E_{pa1}) and at $+620$ mV (E_{pa2}). In the reverse scan, one

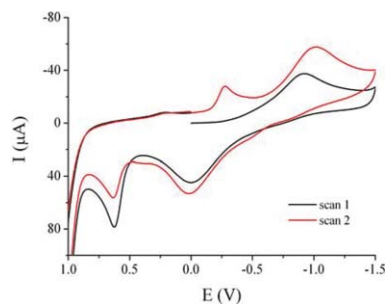


Fig. 7 Cyclic voltammogram of 0.4 mM dmsO solution of **4**. Scan rate = 100 mV s^{-1} . Supporting electrolyte = TEAP, 0.1 M.

Table 5 Cathodic and anodic potentials (in mV) for the redox couples Co(II)/Co(I) and Co(III)/Co(II) in dmsO solution and for the redox couple Co(II)/Co(I) in 1 : 2 dmsO : buffer solution of the complexes in the absence and presence of CT DNA

Complex	E_{pc1}^a	E_{pa1}^a	E_{pa2}^a	E_{pc2}^a	$E_{pc(f)}^b$	$E_{pc(b)}^c$	ΔE_{pc}^d	$E_{pa(f)}^b$	$E_{pa(b)}^c$	ΔE_{pa}^d
[Co(mef) ₂ (MeOH) ₄], 1	−1010	−45	+600	−303	−675	−675	0	−547	−527	+20
[Co(mef) ₂ (bipy)(MeOH) ₂], 2	−1205	−25	+620	−215	−750	−700	+50	−550	−490	+60
[Co(mef) ₂ (phen)(MeOH) ₂], 3	−960	+180	+590	−315	−665	−665	0	−525	−540	−15
[Co(mef) ₂ (py) ₂ (MeOH) ₂], 4	−920	−10	+620	−270	−685	−680	+5	−560	−535	+25

^a $E_{pc/a}$ in dmsO solution. ^b $E_{pc/a}$ in dmsO/buffer in the absence of CT DNA ($E_{pc/a(f)}$). ^c $E_{pc/a}$ in dmsO/buffer in the presence of CT DNA ($E_{pc/a(b)}$). ^d $\Delta E_{pc/a} = E_{pc/a(b)} - E_{pc/a(f)}$.

more cathodic wave appears at -270 mV (E_{pc2}). The one-electron cathodic wave at E_{pc1} can be attributed to the reduction of [Co(II)] to [Co(I)], while the two anodic waves at E_{pa1} and E_{pa2} can be attributed to the oxidation processes [Co(I)] \rightarrow [Co(II)] and [Co(II)] \rightarrow [Co(III)], respectively, with the second cathodic wave at E_{pc2} to the reduction of [Co(III)] to [Co(II)] species.^{17b,c} Complexes **1–3** present similar cyclic voltammograms in dmsO solution and the corresponding potentials are given in Table 5.

The electrochemical investigations of metal–DNA interactions can provide a useful supplement to spectroscopic methods and yield information about interactions with both the reduced and oxidized form of the metal. In general, the electrochemical potential of a small molecule will shift positively when it intercalates into DNA double helix, and it will shift to a negative direction in the case of electrostatic interaction with DNA.³⁰

The quasi-reversible redox couple Co(II)/Co(I) for each complex in 1 : 2 dmsO : buffer solution has been studied upon addition of CT DNA and the corresponding potentials as well as their shifts are given in Table 5. No new redox peaks appeared after the addition of CT DNA to each complex, but the current intensity of all the peaks decreased significantly, suggesting the existence of an interaction between each complex and CT DNA, and can be explained in terms of an equilibrium mixture of free and DNA-bound complex to the electrode surface.^{17b}

For increasing amounts of CT DNA, the cathodic potential E_{pc} for all complexes shows a positive shift ($\Delta E_{pc} = 0 - (+50)$ mV) (Table 5) while the anodic potential E_{pa} shifts slightly to more negative or positive values ($\Delta E_{pa} = (-15) - (+60)$ mV) suggesting an intercalative mode of binding while the co-existence of external (possibly electrostatic) interaction in the case of **3** (negative shift of E_{pa}) cannot be ruled out.^{17b,e,f,30b}

Binding of serum albumins

It is important to consider the interactions of drugs with plasma proteins particularly with serum albumin, which is the most abundant protein in plasma. Binding to these proteins may lead to loss or enhancement of the biological properties of the original drug, or provide paths for drug transportation. Bovine serum albumin (BSA) is the most extensively studied serum albumin, due to its structural homology with human serum albumin (HSA). BSA with its two tryptophans, Trp-134 and Trp-212, and HSA with one Trp-214, can bind reversibly to a large number of endogenous and exogenous compounds.³¹ The interaction of Hmef and complexes **1–4** with serum albumins has been studied from tryptophan emission-quenching experiments. BSA and HSA solutions exhibit a strong fluorescence emission with a peak at

Table 6 The BSA binding constants and parameters (K_{sv} , k_q , K , n) derived for Hmef and complexes **1–4**

Compound	K_{sv}/M^{-1}	$k_q/M^{-1} s^{-1}$	K/M^{-1}	n
Hmef	$2.78 (\pm 0.20) \times 10^5$	$2.78 (\pm 0.20) \times 10^{13}$	1.35×10^5	1.20
[Co(mef) ₂ (MeOH) ₄], 1	$2.11 (\pm 0.22) \times 10^6$	$2.11 (\pm 0.22) \times 10^{14}$	2.22×10^5	1.27
[Co(mef) ₂ (bipy)(MeOH) ₂], 2	$2.86 (\pm 0.23) \times 10^6$	$2.86 (\pm 0.23) \times 10^{14}$	2.38×10^5	1.31
[Co(mef) ₂ (phen)(MeOH) ₂], 3	$6.04 (\pm 0.25) \times 10^5$	$6.04 (\pm 0.25) \times 10^{13}$	3.66×10^5	1.06
[Co(mef) ₂ (py) ₂ (MeOH) ₂], 4	$6.32 (\pm 0.37) \times 10^5$	$6.32 (\pm 0.37) \times 10^{13}$	2.37×10^5	1.12

343 nm and 351 nm, respectively, due to their tryptophan residues, when excited at 295 nm. The changes in the emission spectra of tryptophan in BSA or HSA are primarily due to change in protein conformation, subunit association, substrate binding or denaturation,^{31b} since Hmef and complexes **1–4** in buffer solutions do not exhibit any emission spectra under the same experimental conditions.

Addition of Hmef or complexes **1–4** to BSA results in a significant decrease of the fluorescence (up to 10% of the initial fluorescence intensity of BSA for Hmef (Fig. 8), 2% for **1**, 1% for **2**, 6% for **3** and 7% for **4**) at $\lambda = 343$ nm without any other spectroscopic changes due to possible changes in protein secondary structure of BSA indicating the binding of Hmef or each complex to BSA.

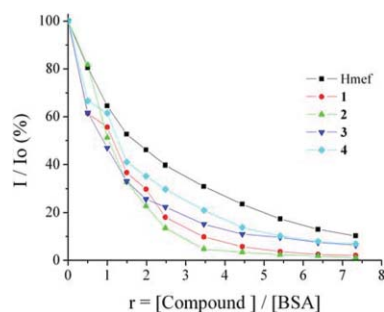


Fig. 8 Plot of % relative fluorescence intensity at $\lambda_{em} = 342$ nm (%) versus r ($r = [\text{compound}]/[\text{BSA}]$) for Hmef and complexes **1–4** in buffer solution (150 mM NaCl and 15 mM trisodium citrate at pH 7.0).

The Stern–Volmer and Scatchard graphs may be used in order to study the interaction of a quencher in presence of serum albumins. According to Stern–Volmer quenching equation:³²

$$\frac{I_0}{I} = 1 + k_q \tau_0 [Q] = 1 + K_{SV} [Q] \quad (5)$$

where I_0 = the initial tryptophan fluorescence intensity of SA, I = the tryptophan fluorescence intensity of SA after the addition of the quencher, k_q = the quenching rate constant SA, K_{sv} = the dynamic quenching constant, τ_0 = the average lifetime of SA without the quencher, $[Q]$ = the concentration of the quencher respectively and $K_{sv} = k_q \tau_0$, and taking the fluorescence lifetime (τ_0) of tryptophan in SA at around 10^{-8} s,³² the dynamic quenching constant (K_{sv} , M^{-1}) can be obtained by the slope of the diagram $\frac{I_0}{I}$ versus $[Q]$ (Fig. S3†), and subsequently the approximate quenching constant (k_q , $M^{-1} s^{-1}$) may be calculated. The calculated values of K_{sv} and k_q ($\tau_0 \sim 10^{-8}$ s) for the interaction of Hmef and complexes **1–4** with BSA are given in Table 6 and indicate good BSA binding propensity of the complexes. Complex **2** exhibits the

strongest protein-binding ability ($k_q = 2.86 (\pm 0.23) \times 10^{14}$) since k_q increases in the order Hmef $< 3 < 4 < 1 < 2$ with values ($> 10^{13} M^{-1} s^{-1}$) higher than the diverse kinds of quenchers for biopolymer fluorescence ($2.0 \times 10^{10} M^{-1} s^{-1}$) indicating the existence of static quenching mechanism.^{31c} Similar k_q values (10^{12} – $10^{13} M^{-1} s^{-1}$) have been recently reported for a series of Ni(II) and Zn(II) complexes with quinolone antibacterial agents, where the complexes have exhibited higher affinity to human or bovine serum albumin than the free drug.^{17e–h}

Using the Scatchard equation:³³

$$\frac{\Delta I}{I_0} = nK - K \frac{\Delta I}{I_0} \quad (6)$$

where n is the number of binding sites per albumin and K is the association binding constant, K (M^{-1}) may be calculated from the slope in plots $\frac{\Delta I}{I_0}$ versus $\frac{\Delta I}{I_0}$ (Fig. S4†) and n is given by the ratio of the y intercept to the slope.³³ The K and n values are cited in Table 6 with **3** having the highest K value and **2** the highest n value. The K values are relatively high and Hmef exhibits the lowest value, indicating that its coordination to Co^{2+} leads to enhanced stability of the corresponding compound with BSA. The n values of all compounds are of similar magnitude (1.06–1.30) with **2** showing the highest value.

The quenching provoked by Hmef or complexes **1–4** to the HSA fluorescence at $\lambda = 351$ nm (Fig. 9) is significant (up to 40% of the initial fluorescence intensity for Hmef, 17% for **1**, 13% for **2**, 12% for **3** and 28% for **4**) without any other spectroscopic changes indicating that the binding of the compounds to HSA quenches the intrinsic fluorescence of the single tryptophan in HSA.³⁴

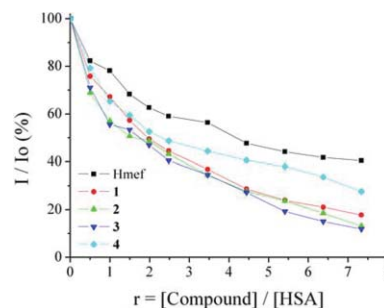


Fig. 9 Plot of % relative fluorescence intensity at $\lambda_{em} = 352$ nm (%) versus r ($r = [\text{compound}]/[\text{HSA}]$) for Hmef and complexes **1–4** in buffer solution (150 mM NaCl and 15 mM trisodium citrate at pH 7.0).

The calculated values of K_{sv} and k_q , as obtained by the slope of the Stern–Volmer plot (Fig. S5†), for Hmef and **1–4** are given in Table 7 and indicate their good HSA binding propensity. The k_q

Table 7 The HSA binding constants (K_{sv} , k_q , K , n) derived for Hmef and complexes **1–4**

Compound	K_{sv}/M^{-1}	$k_q/M^{-1} s^{-1}$	K/M^{-1}	n
Hmef	$7.13 (\pm 0.34) \times 10^4$	$7.13 (\pm 0.34) \times 10^{12}$	1.32×10^5	0.82
[Co(mef) ₂ (MeOH) ₄], 1	$1.96 (\pm 0.06) \times 10^5$	$1.96 (\pm 0.06) \times 10^{13}$	1.46×10^5	1.07
[Co(mef) ₂ (bipy)(MeOH) ₂], 2	$1.88 (\pm 0.08) \times 10^5$	$1.88 (\pm 0.08) \times 10^{13}$	1.34×10^5	1.13
[Co(mef) ₂ (phen)(MeOH) ₂], 3	$2.29 (\pm 0.20) \times 10^5$	$2.29 (\pm 0.20) \times 10^{13}$	1.49×10^5	1.13
[Co(mef) ₂ (py) ₂ (MeOH) ₂], 4	$1.03 (\pm 0.06) \times 10^5$	$1.03 (\pm 0.06) \times 10^{13}$	2.43×10^5	0.79

values increase in the order Hmef < **4** < **2** < **1** < **3**, with complex **3** exhibiting the strongest protein-binding ability and provoking the highest quenching. The k_q values ($>10^{13} M^{-1} s^{-1}$) are similar to those observed for Ni(II) and Zn(II) quinolone complexes^{17e-h} and are higher than diverse quenchers for biopolymers fluorescence ($2.0 \times 10^{10} M^{-1} s^{-1}$) suggesting a static quenching mechanism.

From the Scatchard plot (Fig. S6†) and eqn (6),³⁴ the K and n values of each compound have been calculated (Table 7). All the complexes have similar K values to that of Hmef except **4** which exhibits the highest association binding constant to HSA ($2.43 \times 10^5 M^{-1}$), while the n values of complexes **1–3** are higher than that of Hmef with **2** and **3** having the highest n value (~ 1.13).

Comparing the affinity of Hmef and complexes **1–4** for BSA and HSA (K values), it is obvious that **1–3** show higher affinity for BSA than HSA, while mefenamic acid and **1**, the corresponding K_A constants present similar values. Additionally, the affinity of mefenamic acid is enhanced when coordinated in all complexes **1–4**.

Antioxidant capacity

Free radicals play an important role in the inflammatory process as it is known. Many NSAIDs with a broad spectrum of effects have been reported to act either as inhibitors of free radical production or as radical scavengers.³⁵ Thus, compounds with possible antioxidant properties could play a crucial role against inflammation and lead to potentially effective drugs. The compounds were tested in comparison to well-known antioxidant agents *e.g.* nordihydroguaiaretic acid (NDGA), butylated hydroxytoluene (BHT) and 6-hydroxy-2,5,7,8-tetramethylchromane-2-carboxylic acid (Trolox). In this context, Hmef and complexes **1–4** have been tested with regard to their antioxidant ability and the results are shown in Tables 8 and 9.

Antioxidants that exhibit 1,1-diphenyl-picrylhydrazyl (DPPH) radical scavenging activity are receiving increased attention since they present interesting anticancer, anti-ageing and anti-inflammatory activities.^{36a} Therefore, compounds with antioxidant properties may offer protection in rheumatoid arthritis

Table 8 Interaction % with DPPH (RA%)

	20 min, 0.1 mM	60 min, 0.1 mM
Hmef	5.7	11.7
[Co(mef) ₂ (MeOH) ₄], 1	29.9	30.1
[Co(mef) ₂ (bipy)(MeOH) ₂], 2	20.4	17.9
[Co(mef) ₂ (phen)(MeOH) ₂], 3	32.5	36.8
[Co(mef) ₂ (py) ₂ (MeOH) ₂], 4	28.6	29.5
NDGA	81	82.6
BHT	31.3	60

Each experiment was performed at least in triplicate SD < $\pm 10\%$.

Table 9 Competition % with DMSO for hydroxyl radical ($\cdot OH\%$); % superoxide radical scavenging activity (ABTS%)

	$\cdot OH\%$ 0.1 mM	ABTS% 0.1 mM
Hmef	92.5	66.3
[Co(mef) ₂ (MeOH) ₄], 1	95.7	78.3
[Co(mef) ₂ (bipy)(MeOH) ₂], 2	96.4	92.4
[Co(mef) ₂ (phen)(MeOH) ₂], 3	89.3	90.4
[Co(mef) ₂ (py) ₂ (MeOH) ₂], 4	96.7	97.0
Trolox	88.2	91.8

Each experiment was performed at least in triplicate SD < $\pm 10\%$.

and inflammation. DPPH is a stable free radical and presents strong absorption band at 517 nm. The interaction of Hmef and complexes **1–4** with the stable free radical DPPH (Table 8) has revealed their reducing activity. The measurements were performed after 20 and 60 min. In general, the tested compounds present low to moderate interaction values. The order of the reducing activity of the compounds increases in the order Hmef < **2** < **4** < **1** < **3**. Complexes **2**, **3** and **4** containing a lipophilic moiety (bipy, phen and py respectively) showed low reducing activity. **1** and **3** seem to be the most active and their activity is not time dependent.

Hydroxyl radicals are characterized aiming the most reactive oxygen species. During the inflammatory process, phagocytes generate the superoxide anion radical at the inflamed site, and this is connected to other oxidizing species such as $OH\cdot$.^{36b} They are considered to be responsible for some of the tissue damage occurring in inflammation. It is claimed that hydroxyl radical scavengers could serve as protectors, thus increasing prostaglandin synthesis. The competition of the new complexes with DMSO for $HO\cdot$, generated by the Fe^{3+} /ascorbic acid system, expressed as percent inhibition of formaldehyde production, has been used for the evaluation of their hydroxyl radical scavenging activity and the results are cited in Table 9. All the compounds are found to present strong competition with DMSO (33 mM) at 0.1 mM for hydroxyl free radicals. Hmef shows significant scavenging activity (92.5%) and complexes **1**, **2** and **4** present even higher scavenging activity. The hydroxyl radical scavenging activity increases in the order **3** < Hmef < **1** < **2** < **4**.

Generation of the 2,2'-azinobis-(3-ethylbenzothiazoline-6-sulfonic acid) (ABTS) radical cation forms the basis of one of the spectrophotometric methods applied to the measurement of the total antioxidant activity of solutions of Hmef and **1–4**.^{36c} Hmef presents a rather high activity (66.3%) while complexes **1–4** present a much higher activity increasing in the order Hmef < **1** < **3** < **2** < **4** (Table 9). All the complexes are more potent than mefenamic acid. The activity of mefenamic acid is enhanced when coordinated to Co(II) in **1** (78.3%), while in the presence of

the N,N'-donor ligands phen and bipy the activity increases even more (90.4% and 92.4% respectively) and especially in the presence of py in **4** (97.0%) which presents the highest activity.

In conclusion, all the complexes exhibit higher inhibition than mefenamic acid against the DPPH and ABTS radicals. The inhibition of all the compounds against hydroxyl radicals is very high, with complexes **1**, **2** and **4** showing better inhibition than mefenamic acid. In the literature, diverse Cu(II), Co(II), Ni(II), Zn(II) and Pd(II) complexes with drugs or Schiff bases as ligands have presented enhanced antioxidant activity in relation to the free ligands.^{36b,37}

Conclusions

The synthesis and characterization of neutral mononuclear cobalt(II) complexes with the non-steroidal anti-inflammatory drug mefenamic acid in the absence or presence of a nitrogen donor heterocyclic ligand 2,2'-bipyridine, 1,10-phenanthroline or pyridine has been achieved. In these complexes, the mefenamate ligand is bound to cobalt(II) via a carboxylato oxygen. [Co(mef)₂(bipy)(MeOH)₂] and centrosymmetric [Co(mef)₂(MeOH)₄] present a distorted octahedral geometry around the cobalt atom. EPR signals of **1** and **2** reveal an octahedral geometry of the Co(II) ion. Complexes **1** and **2** are the first cobalt(II) complexes of the NSAID anthranilic acids that have been structurally characterized.

UV spectroscopy and cyclic voltammetry studies have revealed the ability of the complexes to bind to DNA. The binding strength of the complexes with CT DNA calculated with UV spectroscopic titrations have shown that [Co(mef)₂(MeOH)₄] exhibits the highest K_b value among the compounds examined. Competitive binding studies with EB have revealed the ability of the complexes to displace EB from the EB-DNA complex and cyclic voltammetry studies have confirmed the intercalation as the most possible binding mode to DNA.

The complexes show good binding affinity to BSA and HSA proteins giving relatively high binding constants. All the compounds were tested *in vitro* for their antioxidant and free radical scavenging activity. They present significantly high scavenging activity against hydroxyl free radicals and superoxide radicals with **4** being the most active one.

Experimental

Materials and instrumentation

Mefenamic acid, CT DNA, BSA, HSA, EB, DPPH, ABTS, Trolox and caffeic acid were purchased from Sigma, NaCl and all solvents were purchased from Merck, trisodium citrate was purchased from Riedel-de Haen and CoCl₂·6H₂O, bipy, phen, py, KOH and NDGA were purchased from Aldrich Co. All the chemicals and solvents were reagent grade and were used as purchased. Tetraethylammonium perchlorate (TEAP) was purchased from Carlo Erba and, prior to its use, it was recrystallized twice from ethanol and dried under vacuum.

DNA stock solution was prepared by dilution of CT DNA to buffer (containing 15 mM trisodium citrate and 150 mM NaCl at pH 7.0) followed by exhaustive stirring for three days, and kept at 4 °C for no longer than a week. The stock solution of CT DNA

gave a ratio of UV absorbance at 260 and 280 nm (A_{260}/A_{280}) of 1.89, indicating that the DNA was sufficiently free of protein contamination.³⁸ The DNA concentration was determined by the UV absorbance at 260 nm after 1:20 dilution using $\epsilon = 6600 \text{ M}^{-1}\text{cm}^{-1}$.³⁹

Infrared (IR) spectra (400–4000 cm⁻¹) were recorded on a Nicolet FT-IR 6700 spectrometer with samples prepared as KBr disk. UV-visible (UV-vis) spectra were recorded as nujol mulls and in solution at concentrations in the range 10⁻⁵–10⁻³ M on a Hitachi U-2001 dual beam spectrophotometer. Room temperature magnetic measurements were carried out by the Faraday method using mercury tetrathiocyanatocobaltate(II) as a calibrant. C, H and N elemental analysis were performed on a Perkin-Elmer 240B elemental analyzer. Molecular conductivity measurements were carried out with a Crison Basic 30 conductometer. Fluorescence spectra were recorded in solution on a Hitachi F-7000 fluorescence spectrophotometer. Solid state and solution EPR measurements were taken in the temperature range 4–300 K on a Bruker 200D-SRC X-Band spectrometer, equipped with an Oxford ESR 9 Cryostat, operating at 9.412 GHz, 10 db.

Cyclic voltammetry studies were performed on an Eco chemie Autolab Electrochemical analyzer. Cyclic voltammetry experiments were carried out in a 30 mL three-electrode electrolytic cell. The working electrode was platinum disk, a separate Pt single-sheet electrode was used as the counter electrode and a Ag/AgCl electrode saturated with KCl was used as the reference electrode. The cyclic voltammograms of the complexes were recorded in 0.4 mM dmsO solutions and in 0.4 mM 1:2 dmsO:buffer solutions at $\nu = 100 \text{ mV s}^{-1}$ where TEAP and the buffer solution were the supporting electrolytes, respectively. Oxygen was removed by purging the solutions with pure nitrogen which had been previously saturated with solvent vapours. All electrochemical measurements were performed at 25.0 ± 0.2 °C.

Synthesis of the complexes

[Co(mef)₂(MeOH)₄]·2MeOH, 1·2MeOH. A methanolic solution (15 mL) containing mefenamic acid (0.4 mmol, 97 mg) and KOH (0.4 mmol, 22 mg) was stirred for 1 h. The solution was added to a methanolic solution (10 mL) of CoCl₂·6H₂O (0.2 mmol, 48 mg) and the reaction mixture was stirred for 1 h. The reaction solution was filtered and left for slow evaporation. Rose-colored crystals of [Co(mef)₂(MeOH)₄]·2MeOH, 1·2MeOH, (105 mg, 75%) suitable for X-ray structure determination, were deposited after a few days. (Found: C, 59.09; H, 7.16; N, 3.83. C₃₆H₅₂CoN₂O₁₀ (MW = 731.75) requires C, 59.75; H, 6.92; N, 4.00%). IR: $\nu_{\text{max}}/\text{cm}^{-1}$; $\nu_{\text{asym}}(\text{CO}_2)$, 1615 (vs (very strong)); $\nu_{\text{sym}}(\text{CO}_2)$, 1389 (vs); $\Delta = \nu_{\text{asym}}(\text{CO}_2) - \nu_{\text{sym}}(\text{CO}_2)$: 226 cm⁻¹ (KBr disk); UV-vis: λ/nm ($\epsilon/\text{M}^{-1}\text{cm}^{-1}$) as nujol mull: 720, 541, 454, 396, 350, 289; in dmsO: 742 (53), 558 (40), 453 (sh (shoulder)) (54), 394 (230), 340 (2300), 292 (5300). $\mu_{\text{eff}} = 4.40 \text{ BM}$. The complex is soluble in dmsO, dmf, CH₂Cl₂, CHCl₃ and ethanol and is non-electrolyte.

[Co(mef)₂(bipy)(MeOH)₂], 2. Mefenamic acid (0.4 mmol, 97 mg) was dissolved in methanol (15 mL) followed by the addition of KOH (0.4 mmol, 22 mg). After 1 h stirring, the resultant solution was added slowly, and simultaneously with a methanolic solution of bipy (0.2 mmol, 31 mg), to a methanolic solution (10 mL) of CoCl₂·6H₂O (0.2 mmol, 48 mg) and stirred for 30 min.

The solution was left for slow evaporation. Orange crystals of [Co(mef)₂(bipy)(MeOH)₂], **2** (105 mg, 70%) suitable for X-ray structure determination, were deposited after a few days. (Found: C, 66.65; H, 5.91; N, 7.53. C₄₂H₄₄CoN₄O₆ (MW = 759.77) requires C, 66.40; H, 5.84; N, 7.37%). IR: $\nu_{\max}/\text{cm}^{-1}$; $\nu_{\text{asym}}(\text{CO}_2)$: 1609 (vs); $\nu_{\text{sym}}(\text{CO}_2)$: 1382 (vs); $\Delta = \nu_{\text{asym}}(\text{CO}_2) - \nu_{\text{sym}}(\text{CO}_2)$: 227 cm⁻¹ (KBr disk); UV-vis: λ/nm ($\epsilon/\text{M}^{-1}\text{cm}^{-1}$) as nujol mull: 745, 550, 480 (sh), 394, 356, 297; in dmsO: 740 (50), 565 (25), 475 (40), 395 (sh) (290), 355 (9800), 295 (11 000). $\mu_{\text{eff}} = 4.46$ BM. The complex is soluble in dmsO and dmF and is non-electrolyte.

[Co(mef)₂(phen)(MeOH)₂], **3**. Complex **3** (100 mg, 65%) was prepared by the addition of a methanolic solution (15 mL) of Hmef (0.4 mmol, 97 mg) and KOH (0.4 mmol, 22 mg), which was stirred for 30 min, and of a methanolic solution of phen (0.2 mmol, 36 mg) to a methanolic solution (10 mL) of CoCl₂·6H₂O (0.2 mmol, 48 mg). The brownish microcrystalline product was collected after a few days. (Found C, 67.75; H, 5.51; N, 7.32; C₄₄H₄₄CoN₄O₆ (MW = 783.79) requires C, 67.43; H, 5.66; N, 7.15%). IR: $\nu_{\max}/\text{cm}^{-1}$; $\nu_{\text{asym}}(\text{CO}_2)$: 1615 (vs); $\nu_{\text{sym}}(\text{CO}_2)$: 1385 (vs); $\Delta = \nu_{\text{asym}}(\text{CO}_2) - \nu_{\text{sym}}(\text{CO}_2)$: 230 cm⁻¹ (KBr disk); UV-vis: λ/nm ($\epsilon/\text{M}^{-1}\text{cm}^{-1}$) as nujol mull: 695, 520, 445 (sh), 405, 355, 295; in dmsO: 735 (40), 550 (25), 460 (50), 398 (110), 352 (2800), 292 (5300). $\mu_{\text{eff}} = 4.35$ BM. The complex is soluble in dmsO and dmF and is non-electrolyte.

[Co(mef)₂(py)₂(MeOH)₂], **4**. The complex was prepared by the addition of a methanolic solution (15 mL) of Hmef (0.4 mmol, 97 mg) and KOH (0.4 mmol, 22 mg), after 30 min of stirring, to a methanolic solution (10 mL) of CoCl₂·6H₂O (0.2 mmol, 48 mg) followed by the addition of 1.5 mL of pyridine. The rose-colored microcrystalline product (105 mg, 70%) was collected after a few days. (Found C, 65.97; H, 6.21; N, 7.31; C₄₂H₄₆CoN₄O₆ (MW = 761.76) requires C, 66.22; H, 6.09; N, 7.36%). IR: $\nu_{\max}/\text{cm}^{-1}$; $\nu_{\text{asym}}(\text{CO}_2)$: 1612 (vs); $\nu_{\text{sym}}(\text{CO}_2)$: 1388 (vs); $\Delta = \nu_{\text{asym}}(\text{CO}_2) - \nu_{\text{sym}}(\text{CO}_2)$: 224 cm⁻¹ (KBr disk); UV-vis: λ/nm ($\epsilon/\text{M}^{-1}\text{cm}^{-1}$) as nujol mull: 690, 510, 445 (sh), 390, 342, 295; in dmsO: 733 (53), 535 (25), 440 (sh) (30), 395 (320), 340 (3200), 293 (6750). $\mu_{\text{eff}} = 4.50$ BM. The complex is soluble in dmsO, CH₂Cl₂ and CHCl₃, and is non-electrolyte.

DNA-binding studies

The interaction of Hmef and complexes **1–4** with CT DNA has been studied with UV spectroscopy in order to investigate the possible binding modes to CT DNA and to calculate the binding constants to CT DNA (K_b). In UV titration experiments, the spectra of CT DNA in the presence of each compound have been recorded for a constant CT DNA concentration in diverse [compound]/[CT DNA] mixing ratios (r). The binding constants, K_b , of the compounds with CT DNA have been determined using the UV spectra of the compound recorded for a constant concentration in the absence or presence of CT DNA for diverse r values. Control experiments with DMSO were performed and no changes in the spectra of CT DNA were observed.

The competitive studies of each compound with EB have been investigated with fluorescence spectroscopy in order to examine whether the compound can displace EB from its CT DNA-EB complex. The CT DNA-EB complex was prepared by adding 20 μM EB and 26 μM CT DNA in buffer (150 mM NaCl and 15 mM

trisodium citrate at pH 7.0). The intercalating effect of Hmef and complexes **1–4** with the DNA-EB complex was studied by adding a certain amount of a solution of the compound step by step into the solution of the DNA-EB complex. The influence of the addition of each compound to the DNA-EB complex solution has been obtained by recording the variation of fluorescence emission spectra.

The interaction of complexes **1–4** with CT DNA has been also investigated by monitoring the changes observed in the cyclic voltammogram of a 0.40 mM 1:2 dmsO:buffer solution of complex upon addition of CT DNA at diverse r values. The buffer was also used as the supporting electrolyte and the cyclic voltammograms were recorded at $\nu = 100$ mV s⁻¹.

Albumin binding studies

The protein binding study was performed by tryptophan fluorescence quenching experiments using bovine (BSA, 3 μM) or human serum albumin (HSA, 3 μM) in buffer (containing 15 mM trisodium citrate and 150 mM NaCl at pH 7.0). The quenching of the emission intensity of tryptophan residues of BSA at 343 nm or HSA at 351 nm was monitored using Hoxo or complexes **1–4** as quenchers with increasing concentration.³² Fluorescence spectra were recorded from 300 to 500 nm at an excitation wavelength of 296 nm.

Antioxidant biological assay

In the *in vitro* assays each experiment was performed at least in triplicate and the standard deviation of absorbance was less than 10% of the mean.

Determination of the reducing activity of the stable radical DPPH

To a solution of DPPH (0.1 mM) in absolute ethanol an equal volume of the compounds dissolved in ethanol was added. As control solution ethanol was used. The concentrations of the solutions of the compounds were 0.05 mM and 0.1 mM. After 20 and 60 min at room temperature, the absorbance at $\lambda = 517$ nm was recorded.^{36a} NDGA and BHT were used as reference compounds.

Competition of the tested compounds with DMSO for hydroxyl radicals

The hydroxyl radicals generated by the Fe³⁺/ascorbic acid system, were detected according to Nash, by the determination of formaldehyde produced from the oxidation of DMSO. The reaction mixture contained EDTA (0.1 mM), Fe³⁺ (167 μM), DMSO (33 mM) in phosphate buffer (50 mM, pH 7.4), the tested compounds (concentration 0.1 mM) and ascorbic acid (10 mM). After 30 min of incubation (37 °C) the reaction was stopped with CCl₃COOH (17% w/v) and the absorbance at $\lambda = 412$ nm was measured.^{36b} Trolox was used as an appropriate standard.

Assay of radical cation scavenging activity

ABTS was dissolved in water to a 2 mM concentration. ABTS radical cation (ABTS^{•+}) was produced by reacting ABTS stock solution with 0.17 mM potassium persulfate and allowing the mixture to stand in the dark at room temperature for 12–16 h before use. Because ABTS and potassium persulfate react

Table 10 Crystallographic data for complexes **1**·2MeOH and **2**

	1 ·2MeOH	2
Formula	C ₃₆ H ₅₂ CoN ₂ O ₁₀	C ₄₂ H ₄₄ CoN ₄ O ₆
Fw	731.73	759.74
Space group	P $\bar{1}$	Ic2a
a/Å	7.66020(10)	7.21870(10)
b/Å	7.88870(10)	17.6361(3)
c/Å	15.7633(3)	29.6060(5)
α /°	90.2790(10)	90
β /°	99.2940(10)	90
γ /°	92.7690(10)	90
V/Å ³	938.88(2)	3769.13(10)
Z	1	4
T/°C	-93	-93
Radiation	Cu K α 1.54178	Cu K α 1.54178
ρ_c /g cm ⁻³	1.294	1.339
μ /mm ⁻¹	4.053	4.003
R ₁ , wR ₂ ^a	0.0523/0.1344 ^b	0.0351/0.0689 ^c

^a $w = 1/[\sigma^2(F_o^2) + (aP)^2 + bP]$ and $P = (\max(F_o^2, 0) + 2F_c^2)/3$, $R1 = \sum(|F_o| - |F_c|)/\sum(|F_o|)$ and $wR2 = \{\sum[w(F_o^2 - F_c^2)^2]/\sum[w(F_o^2)^2]\}^{1/2}$.
^b For 2743 reflections with $I > 2\sigma(I)$. ^c For 2295 reflections with $I > 2\sigma(I)$.

stoichiometrically at a ratio of 1 : 0.5, this will result in incomplete oxidation of the ABTS. Oxidation of the ABTS commenced immediately, but the absorbance was not maximal and stable until more than 6 h had elapsed. The radical was stable in this form for more than 2 days when stored in the dark at room temperature. The ABTS^{•+} solution was diluted with ethanol to an absorbance of 0.70 at $\lambda = 734$ nm. After addition of 10 μ L of diluted compounds or standards (0.1 mM) in DMSO, the absorbance reading was taken exactly 1 min after initial mixing.^{36c}

X-Ray determination

A pink crystal of **1**·2MeOH (0.31 \times 0.67 \times 0.75 mm) and a pink crystal of **2** (0.10 \times 0.27 \times 0.31 mm) were taken from the mother liquor and immediately cooled to -93 °C. Diffraction measurements were made on a Rigaku R-AXIS SPIDER Image Plate diffractometer using graphite monochromated Cu K α radiation. Data collection (ω -scans) and processing (cell refinement, data reduction and Empirical absorption correction) were performed using the CrystalClear program package.⁴⁰ The structures were solved by direct methods using⁴¹ SHELXS-97 and refined by full-matrix least-squares techniques on F^2 with SHELXL-97.⁴² Further experimental crystallographic details for **1**·2MeOH (Table 10): $2\theta_{\max} = 130^\circ$; reflections collected/unique/used, 11 946/2968 [$R_{\text{int}} = 0.0294$]/2968; 270 parameters refined; $(\Delta/\sigma)_{\max} = 0.002$; $(\Delta\rho)_{\max}/(\Delta\rho)_{\min} = 0.725/-0.673$ e/Å³; $R1/wR2$ (for all data), 0.0550/0.1365. Further experimental crystallographic details for **2** (Table 10): $2\theta_{\max} = 126^\circ$; reflections collected/unique/used, 20 358/2940 [$R_{\text{int}} = 0.0399$]/2940; 295 parameters refined; $(\Delta/\sigma)_{\max} = 0.002$; $(\Delta\rho)_{\max}/(\Delta\rho)_{\min} = 0.234/-0.229$ e/Å³; $R1/wR2$ (for all data), 0.0566/0.0818. All hydrogen atoms in both structures either were located by difference maps and were refined isotropically or were introduced at calculated positions as riding on bonded atoms. All non-hydrogen atoms in **1** and **2** were refined anisotropically.

References

1 C. P. Duffy, C. J. Elliott, R. A. O'Connor, M. M. Heenan, S. Coyle, I. M. Cleary, K. Kavanagh, S. Verhaegen, C. M. O'Loughlin,

- R. NicAmhlaibh and M. Clynes, *Eur. J. Cancer*, 1998, **34**, 1250–1259.
- 2 (a) A. R. Amin, P. Vyas, M. Attur, J. Leszczynskapiziak, I. R. Patel, G. Weissmann and S. B. Abramson, *Proc. Natl. Acad. Sci. U. S. A.*, 1995, **92**, 7926–7930; (b) M. Smith, G. Hawcroft and M. A. Hull, *Eur. J. Cancer*, 2000, **36**, 664–674.
- 3 (a) K. Kim, J. Yoon, J. Kim, S. J. Baek, T. E. Eling, W. Lee, J. Ryu, J. Lee, J. Lee and J. Yoo, *Biochem. Biophys. Res. Commun.*, 2004, **325**, 1298–1303; (b) B. Reddy, C. Rao, A. Rivenson and G. Kelloff, *Carcinogenesis*, 1993, **14**, 1493–1497.
- 4 T. Zhang, T. Otevrel, Z. Gao, Z. Gao, S. M. Ehrlich, J. Z. Fields and B. M. Boman, *Cancer Res.*, 2001, **61**, 8664–8667.
- 5 (a) J. F. Neault, M. Naoui, M. Manfait and H. A. Tajmir-Riahi, *FEBS Lett.*, 1996, **382**, 26–30; (b) S. Roy, R. Banerjee and M. Sarkar, *J. Inorg. Biochem.*, 2006, **100**, 1320–1331.
- 6 J. E. Weder, C. T. Dillon, T. W. Hambley, B. J. Kennedy, P. A. Lay, J. R. Biffin, H. L. Regtop and N. M. Davies, *Coord. Chem. Rev.*, 2002, **232**, 95–126 and references therein.
- 7 (a) F. T. Greenaway, E. Riviere, J. J. Girerd, X. Labouze, G. Morgant, B. Viostat, J. C. Daran, M. Roch Arveiller and N. Dung, *J. Inorg. Biochem.*, 1999, **76**, 19–27 and references therein; (b) B. Viostat, J. Daran, G. Savouret, G. Morgant, F. T. Greenaway, N. Dung, V. A. Pham-Tran and J. R. J. Sorenson, *J. Inorg. Biochem.*, 2003, **96**, 375–385 and references therein.
- 8 (a) V. Dokorou, Z. Ciunik, U. Russo and D. Kovala-Demertzi, *J. Organomet. Chem.*, 2001, **630**, 205–214; (b) S. Lorinc, M. Koman, M. Melnik and M. Jaroslava, *Acta Crystallogr., Sect. E: Struct. Rep. Online*, 2006, **62**, m1938–m1939; (c) G. Facchin, M. H. Torre and E. J. Baran, *Z. Naturforsch. Teil B*, 1998, **53**, 871–874.
- 9 P. V. Bernhardt and G. A. Lawrance, in *Comprehensive Coordination Chemistry II*, ed. J. A. McCleverty and T. J. Meyer, 2003, vol. 6, ch. 1, pp. 1–45.
- 10 P. J. Sadler, *Adv. Inorg. Chem.*, 1991, **36**, 1–48.
- 11 (a) M. D. Hall, T. W. Failes, N. Yamamoto and T. W. Hambley, *Dalton Trans.*, 2007, 3983–3990; (b) F. P. Dwyer, E. C. Gyrfas, W. P. Rogers and J. H. Koch, *Nature*, 1952, **170**, 190–191.
- 12 (a) H. Lopez-Sandoval, M. E. Londono-Lemos, R. Garza-Velasco, I. Poblano-Melendez, P. Granada-Macias, I. Gracia-Mora and N. Barba-Behrens, *J. Inorg. Biochem.*, 2008, **102**, 1267–1276; (b) I. Ott, A. Abraham, P. Schumacher, H. Shorafa, G. Gastl, R. Gust and B. Kircher, *J. Inorg. Biochem.*, 2006, **100**, 1903–1906; (c) I. Ott, K. Schmidt, B. Kircher, P. Schumacher, T. Wiglenda and R. Gust, *J. Med. Chem.*, 2005, **48**, 622–629.
- 13 (a) D. U. Miodragovic, G. A. Bogdanovic, Z. M. Miodragovic, M. J. Radulovic, S. B. Novakovic, G. N. Kaludjerovic and H. Kozlowski, *J. Inorg. Biochem.*, 2006, **100**, 1568–1574; (b) K. Nomiya, A. Yoshizawa, K. Tsukagoshi, N. C. Kasuga, S. Hirakawa and J. Watanabe, *J. Inorg. Biochem.*, 2004, **98**, 46–60.
- 14 (a) J. Lv, T. Liu, S. Cai, X. Wang, L. Liu and Y. Wang, *J. Inorg. Biochem.*, 2006, **100**, 1888–1896; (b) Z. Weiqun, Y. Wen, X. Liqun and C. Xianchen, *J. Inorg. Biochem.*, 2005, **99**, 1314–1319.
- 15 (a) A. Bottcher, T. Takeuchi, K. I. Hardcastle, T. J. Meade and H. B. Gray, *Inorg. Chem.*, 1997, **36**, 2498–2504; (b) T. Takeuchi, A. Bottcher, C. M. Quezada, T. J. Meade and H. B. Gray, *Bioorg. Med. Chem.*, 1999, **7**, 815–819.
- 16 (a) C. Dendrinou-Samara, G. Psomas, K. Christophorou, V. Tangoulis, C. P. Raptopoulou, A. Terzis and D. P. Kessissoglou, *J. Chem. Soc., Dalton Trans.*, 1996, 3737–3743; (b) M. Alexiou, I. Tsvikas, C. Dendrinou-Samara, A. Pantazaki, P. Trikalitis, N. Lalioti, D. A. Kyriakidis and D. P. Kessissoglou, *J. Inorg. Biochem.*, 2003, **93**, 256–264; (c) A. Dimitrakopoulou, C. Dendrinou-Samara, A. A. Pantazaki, M. Alexiou, E. Nordlander and D. P. Kessissoglou, *J. Inorg. Biochem.*, 2008, **102**, 618–628.
- 17 (a) G. Psomas, A. Tarushi, E. K. Efthimiadou, Y. Sanakis, C. P. Raptopoulou and N. Katsaros, *J. Inorg. Biochem.*, 2006, **100**, 1764–1773; (b) G. Psomas, *J. Inorg. Biochem.*, 2008, **102**, 1798–1811; (c) E. K. Efthimiadou, A. Karalioti and G. Psomas, *Bioorg. Med. Chem. Lett.*, 2008, **18**, 4033–4037; (d) A. Tarushi, G. Psomas, C. P. Raptopoulou and D. P. Kessissoglou, *J. Inorg. Biochem.*, 2009, **103**, 898–905; (e) K. C. Skyrianou, E. Efthimiadou, V. Psycharis, A. Terzis, D. P. Kessissoglou and G. Psomas, *J. Inorg. Biochem.*, 2009, **103**, 1617–1625; (f) K. C. Skyrianou, F. Peridh, I. Turel, D. P. Kessissoglou and G. Psomas, *J. Inorg. Biochem.*, 2010, **104**, 161–170; (g) E. K. Efthimiadou, A. Karalioti and G. Psomas, *J. Inorg. Biochem.*, 2010, **104**, 455–466; (h) A.

- Tarushi, C. P. Raptopoulou, V. Psycharis, A. Terzis, G. Psomas and D. P. Kessissoglou, *Bioorg. Med. Chem.*, 2010, **18**, 2678–2685.
- 18 (a) C. Dendrinou-Samara, D. P. Kessissoglou, G. E. Manoussakis, D. Mentzafos and A. Terzis, *J. Chem. Soc., Dalton Trans.*, 1990, 959–965; (b) C. Dendrinou-Samara, P. D. Jannakoudakis, D. P. Kessissoglou, G. E. Manoussakis, D. Mentzafos and A. Terzis, *J. Chem. Soc., Dalton Trans.*, 1992, 3259–3264; (c) C. Dendrinou-Samara, G. Tsotsou, C. P. Raptopoulou, A. Kortsaris, D. Kyriakidis and D. P. Kessissoglou, *J. Inorg. Biochem.*, 1998, **71**, 171–179; (d) P. Christofis, M. Katsarou, A. Papakyriakou, Y. Sanakis, N. Katsaros and G. Psomas, *J. Inorg. Biochem.*, 2005, **99**, 2197–2210.
- 19 (a) I. Bertini and C. Luchinat, in *Advances in Inorganic Biochemistry*, ed. G. L. Eichorn and L. G. Marzilli, Elsevier, New York, 1984, vol. 6, pp. 78–80; (b) J. Zarembowitch and O. Kahn, *Inorg. Chem.*, 1984, **23**, 589–593; (c) A. Bencini, C. Benelli, D. Gatteschi and C. Zanchini, *Inorg. Chem.*, 1979, **18**, 2526–2528.
- 20 A. Grirrane, A. Pastor, A. Ienco, C. Mealli and A. Galindo, *J. Chem. Soc., Dalton Trans.*, 2002, 3771–3777.
- 21 (a) M. Melnik, M. Koman and T. Glowiak, *Polyhedron*, 1998, **17**, 1767–1771; (b) B. Viossat, F. T. Greenaway, G. Morgant, J. C. Daran, N. H. Dung and J. R. J. Sorenson, *J. Inorg. Biochem.*, 2005, **99**, 355–367; (c) D. Kovala-Demertzi, A. Galani, M. A. Demertzis, S. Skoulika and C. Kotoglou, *J. Inorg. Biochem.*, 2004, **98**, 358–364; (d) F. Valach, M. Tokarcik, P. Kubinec, M. Melnik and L. Macaskova, *Polyhedron*, 1997, **16**, 1461–1464; (e) M. Melnik, I. Potocnak, I. Macaskova and D. Miklos, *Polyhedron*, 1996, **15**, 2159–2164; (f) D. Kovala-Demertzi, V. N. Dokorou, J. P. Jasinski, A. Opolski, J. Wiecek, M. Zervou and M. A. Demertzis, *J. Organomet. Chem.*, 2005, **690**, 1800–1806; (g) D. Kovala-Demertzi, N. Kourkoumelis, A. Koutsodimou, A. Moukarika, E. Horn and E. R. T. Tiekink, *J. Organomet. Chem.*, 2001, **620**, 194–201.
- 22 Q. Zhang, J. Liu, H. Chao, G. Xue and L. Ji, *J. Inorg. Biochem.*, 2001, **83**, 49–55.
- 23 (a) A. M. Pyle, J. P. Rehmann, R. Meshoyrer, C. V. Kumar, N. J. Turro and J. K. Barton, *J. Am. Chem. Soc.*, 1989, **111**, 3053–3063; (b) H. Chao, W. Mei, Q. Huang and L. Ji, *J. Inorg. Biochem.*, 2002, **92**, 165–170; (c) E. C. Long and J. K. Barton, *Acc. Chem. Res.*, 1990, **23**, 271–273.
- 24 Y. Song, Q. Wu, P. Yang, N. Luan, L. Wang and Y. Liu, *J. Inorg. Biochem.*, 2006, **100**, 1685–1691.
- 25 (a) R. F. Pasternack, E. J. Gibbs and J. J. Villafranca, *Biochemistry*, 1983, **22**, 2406–2414; (b) G. Pratviel, J. Bernadou and B. Meunier, *Adv. Inorg. Chem.*, 1998, **45**, 251–262.
- 26 A. Jancso, L. Nagy, E. Moldrheim and E. Sletten, *J. Chem. Soc., Dalton Trans.*, 1999, 1587–1594.
- 27 (a) W. D. Wilson, L. Ratmeyer, M. Zhao, L. Strekowski and D. Boykin, *Biochemistry*, 1993, **32**, 4098–4104; (b) T. Afrati, A. A. Pantazaki, C. Dendrinou-Samara, C. Raptopoulou, A. Terzis and D. P. Kessissoglou, *Dalton Trans.*, 2010, **39**, 765–775.
- 28 R. F. Pasternack, M. Cacca, B. Keogh, T. A. Stephenson, A. P. Williams and F. J. Gibbs, *J. Am. Chem. Soc.*, 1991, **113**, 6835–6840.
- 29 O. Novakova, H. Chen, O. Vrana, A. Rodger, P. J. Sadler and V. Brabec, *Biochemistry*, 2003, **42**, 11544–11554.
- 30 (a) M. T. Carter and A. J. Bard, *J. Am. Chem. Soc.*, 1987, **109**, 7528–7530; (b) M. T. Carter, M. Rodriguez and A. J. Bard, *J. Am. Chem. Soc.*, 1989, **111**, 8901–8911.
- 31 (a) C. Tan, J. Liu, H. Li, W. Zheng, S. Shi, L. Chen and L. Ji, *J. Inorg. Biochem.*, 2008, **102**, 347–358; (b) Y. Wang, H. Zhang, G. Zhang, W. Tao and S. Tang, *J. Lumin.*, 2007, **126**, 211–218; (c) S. Deepa and A. K. Mishra, *J. Pharm. Biomed. Anal.*, 2005, **38**, 556–563.
- 32 J. R. Lakowicz and G. Weber, *Biochemistry*, 1973, **12**, 4161–4170.
- 33 S. Wu, W. Yuan, H. Wang, Q. Zhang, M. Liu and K. Yu, *J. Inorg. Biochem.*, 2008, **102**, 2026–2034.
- 34 V. Rajendiran, R. Karthik, M. Palaniandavar, H. Stoeckli-Evans, V. S. Periasamy, M. A. Akbarsha, B. S. Srinag and H. Krishnamurthy, *Inorg. Chem.*, 2007, **46**, 8208–8221.
- 35 R. Cini, G. Giorgi, A. Cinquantini, C. Rossi and M. Sabat, *Inorg. Chem.*, 1990, **29**, 5197–5200.
- 36 (a) C. Kontogiorgis and D. Hadjipavlou-Litina, *J. Enzyme Inhib. Med. Chem.*, 2003, **18**, 63–69; (b) D. Panagoulis, E. Pontiki, E. Skeva, C. Raptopoulou, S. Girousi, D. Hadjipavlou-Litina and C. Dendrinou-Samara, *J. Inorg. Biochem.*, 2007, **101**, 623–634; (c) R. Re, N. Pellegrini, A. Proteggente, A. Pannala, M. Yang and C. Rice-Evans, *Free Radical Biol. Med.*, 1999, **26**, 1231–1237.
- 37 (a) Z. D. Petrovic, D. Hadjipavlou-Litina and V. P. Petrovic, *J. Mol. Liq.*, 2009, **144**, 55–58; (b) D. Kovala-Demertzi, D. Hadjipavlou-Litina, A. Primikiri, M. Staninska, C. Kotoglou and M. A. Demertzis, *Chem. Biodiversity*, 2009, **6**, 948–960; (c) Z. Liu, B. Wang, Z. Yang, Y. Li, D. Qin and T. Li, *Eur. J. Med. Chem.*, 2009, **44**, 4477–4484; (d) S. B. Bukhari, S. Memon, M. M. Tahir and M. I. Bhangar, *J. Mol. Struct.*, 2008, **892**, 39–46; (e) E. Pontiki, D. Hadjipavlou-Litina, A. T. Chaviara and C. A. Bolos, *Bioorg. Med. Chem. Lett.*, 2006, **16**, 2234–2237.
- 38 J. Marmur, *J. Mol. Biol.*, 1961, **3**, 208–211.
- 39 M. F. Reichmann, S. A. Rice, C. A. Thomas and P. Doty, *J. Am. Chem. Soc.*, 1954, **76**, 3047–3053.
- 40 Rigaku/MS (2005). *CrystalClear*, Rigaku/MS Inc., The Woodlands, Texas, USA.
- 41 G. M. Sheldrick, *SHELXS-97: Structure Solving Program*, University of Göttingen, Germany, 1997.
- 42 G. M. Sheldrick, *SHELXL-97: Crystal Structure Refinement Program*, University of Göttingen, Germany, 1997.